

Numerical Simulation of Estuarine and River Morphology

Simulation numérique de la morphologie estuarienne et fluviale

H. Jacob Vested¹, Søren Tjerry¹, Bo Brahtz Christensen¹ and Ian M. Dubinski²

DHI

Agern Allé 5, DK 2970 Hoersholm, Denmark¹

Tel. +45 45 16 92 00

141 Union Blvd Ste 425, Lakewood, CO 80228, USA²

E-mail : hjv@dhigroup.com, snt@dhigroup.com, bbc@dhigroup.com, imd@dhigroup.com

Numerical simulations of estuarine and river morphology are extremely complicated. The physics covers time and length scales ranging from second to years and from mm to km. In numerical simulations the time and length scales are defined by the model resolution and sub-grid scales have to be parameterized to be included. Firstly, simulations with a curvilinear model for hydrodynamics and sediment transport and formation of braiding rivers are presented. Secondly, simulations of estuarine morphology dominated by tidal flow and the formation of ebb and flood channels are presented. The conditions for simulation of these morphological features are discussed in relation to initial conditions, model resolution and hydrodynamic phenomena such as secondary flows.

La simulation numérique de la morphologie estuarienne et fluviale est extrêmement compliquée. La physique couvre des échelles de temps et d'espace variant de la seconde à l'année et du mm au km. Dans les simulations numériques, les échelles de temps et d'espace sont définies par la résolution du modèle et les modèles d'échelle inférieure doivent être paramétrés afin d'être inclus. Premièrement, des simulations avec un modèle curviligne pour l'hydrodynamique, le transport sédimentaire et la formation de cours d'eau en tresses sont présentées. Deuxièmement, des simulations de morphologie estuarienne dominée par les courants de marée et de formation de chenaux de marée sont présentées. Les conditions utilisées pour les simulations de ces particularités morphologiques sont discutées, par rapport aux conditions initiales, à la résolution du modèle et aux phénomènes hydrodynamiques tels que les écoulements secondaires.

Key words

Numerical modelling, rivers, estuaries, morphology

I INTRODUCTION

Numerical simulation of river and tidal morphology is complex. The main reason is the strong interrelation among mechanisms that act at different spatial and temporal scales. De Vriend et al. (2000) used the following classifications for these different scales: micro-scale: the level of the smallest scale morphological phenomena associated with water and sediment motion (ripple and dune formation); meso-scale: the level of the main morphological features (channels and shoals); macro-scale: the level at which the meso-scale features interact; and mega-scale: the level at which the principal elements of the entire system interact.

From a modelling point of view the challenge is to construct a numerical model that can integrate from micro-scale to mega-scale and still keep the computational requirements at an acceptable level. Two-dimensional, depth-integrated models have proven to be very effective at simulating river morphology such as developing a braided pattern in wide rivers starting from a plane bed (Enggrob and Tjerry 1998). Hibma (2004) studied the formation of estuarine channel/shoal systems with Delft3D and was able to predict realistic ebb and flood channels.

¹ Corresponding author

Numerical models are today extensively used to predict the morphological impact of a variety of engineering design considerations such as hydraulic structures, barrages and dams, deepening of navigation, and climate change. In order to correctly predict the morphological impact, it is a requirement that the numerical models can reproduce the basic morphological features observed in nature.

In the present paper MIKE 21C, which is a curvilinear version of MIKE 21 designed for morphological simulations, is applied to simulate long term morphological features of both river and estuarine (tidally-forced) systems. The importance of helical flow and bank erosion are discussed. An important aspect is the triggering of the morphological instabilities that leads to formation of channels and shoals. This triggering can be induced by numerical inaccuracies in the solution scheme or by introducing a small perturbation in the initial conditions. The objective is to simulate realistic length scales of the morphological features that do not depend on the numerical, i.e. numerical solution method, time step, and grid resolution. This is demonstrated by simulations of a non-tidal braiding river (Jamuna River, Bangladesh), ebb and flood channels in a schematised tidal estuary (Hibma 2004) and a real estuary (Narmada Estuary, India).

Various variations of model inputs are explored, such as helical flow, sediment transport models, constant or time-varying discharge, flow resistance models, and importance of tidal flow relative to river run-off.

II MODEL DESCRIPTION

MIKE 21C is designed for morphological simulations with full feedback between hydrodynamics and morphology. The model is designed for time-true morphology based on either fully dynamic or quasi-steady hydrodynamic flow description. Tidal conditions are simulated as fully dynamically flow, while rivers with slowly varying hydrographs can be simulated as quasi-steady flow.

The hydrodynamics model solves the Saint-Venant equations in curvilinear coordinates; see Ahmadi et al (2009).

Helical flow is derived from the hydrodynamics via streamline curvature; there is no feedback from helical flow to hydrodynamics, as this is only relevant for small width to depth ratios. The standard helical flow model applies, yielding the helical flow intensity:

$$\tan \delta_s = \frac{2}{\kappa^2} \left(1 - \frac{\sqrt{g}}{\kappa C} \right) \frac{h}{R_s} \quad (1)$$

where δ_s is the angle between direction of the bed shear stress associated with the depth-integrated flow direction and the actual bed shear stress direction, κ is the von Karman constant, h is the water depth, g is the gravitational acceleration, C is the Chezy number, and R_s is the streamline radius of curvature.

Spatial adaptation of the helical flow is taken into account by solving an advection-dispersion equation with the characteristic length scale λ_s (Olesen, 1987):

$$\lambda_s = \frac{1.2hC}{\sqrt{g}} \quad (2)$$

The sediment transport description allows up to 16 fractions, including cohesive and non-cohesive sediment with a substrate model allowing the bed to be defined by 0-16 layers updated dynamically along with the bathymetry via continuity. Non-cohesive sediment is divided into bed-load and suspended load. Bed-load includes effects from helical flow and bed slope. Suspended load also includes helical flow as well as adaptation by solving an advection-dispersion equation. Form resistance can be included to account for bed forms and/or vegetation. Non-cohesive sediment transport can be computed according to Engelund and Hansen (1967), van Rijn (1984), and various other formulas. Cohesive sediment transport follows the classical Krone formulation for deposition and the Partheniades–Ariathurai erosion law.

Bed-load is calculated from the selected formula yielding the bed-load magnitude q_b . The magnitude is then subjected to the helical flow and slope modification in the transverse direction (n):

$$q_{b,n} = q_b \left(\tan \delta_s - G\theta^{-a} \frac{\partial z}{\partial n} \right) \quad (3)$$

where $q_{b,n}$ is the bed-load in the transverse direction, θ is the Shields parameter, z is the bed level, and G and a are model parameters. The default field conditions values for the transverse bed-load parameters are $G=1.25$ and $a=0.5$. In the longitudinal direction (s), only a slope modification applies:

$$q_{b,s} = q_b \left(1 - \alpha_s \frac{\partial z}{\partial s} \right) \quad (4)$$

where $q_{b,s}$ is the longitudinal bed-load and α_s is a model parameter.

The suspended sediment concentration is found from an advection-dispersion equation, applicable to both cohesive and non-cohesive sediment, which only differ in the erosion and deposition functions. This advection-dispersion equation differs from regular advection-dispersion equations by transporting the suspended sediment concentration with a modified flux field in order to account for sediment flow across streamlines, originating from the underlying depth-integrated 3D structure (Galappatti, 1983), here shown for non-cohesive sediment:

$$\frac{\partial hc}{\partial t} + \frac{\partial p'c}{\partial x} + \frac{\partial q'c}{\partial y} = \frac{\partial}{\partial x} \left(hD \frac{\partial c}{\partial x} \right) + \frac{\partial}{\partial y} \left(hD \frac{\partial c}{\partial y} \right) + \gamma w_s (c_{eq} - c) \quad (5)$$

where (p', q') is a modified flux field explained in the following, c is the actual sediment concentration, c_{eq} is the equilibrium sediment concentration corresponding to the suspended sediment transport capacity obtained from the selected formula, D is a dispersion coefficient, h is the water depth, γ is a profile function related to the bed concentration of sediment, and w_s is the settling velocity. The depth-integration yields reduced longitudinal advection due to the sediment concentration and main velocity profiles; and transverse suspended sediment advection due to helical flow that moves suspended sediment towards the local centre of curvature similar to the helical flow impact on bed-load. The advection is described by the modified flux field:

$$\begin{pmatrix} p' \\ q' \end{pmatrix} = \alpha_{01} \begin{pmatrix} p \\ q \end{pmatrix} + \alpha_{02} \frac{h}{R_s} \begin{pmatrix} -q \\ p \end{pmatrix} \quad (6)$$

where α_{01} and α_{02} are profile functions derived from the theoretical velocity and concentration profiles.

The bed level is updated at each morphological time-step by using the Exner equation for the bed-load:

$$(1-n) \frac{\partial z}{\partial t} + \frac{\partial q_{bx}}{\partial x} + \frac{\partial q_{by}}{\partial y} = 0 \quad (7)$$

In the numerical formulation this is solved in conservative form to avoid curvature terms. For the suspended load it is much better to calculate bed level changes from the advection-dispersion equation through the source/sink terms because this avoids inaccuracies associated with sediment accumulation in the water column, particularly for fine sediment.

The flow resistance can be set to a Manning's ($M=1/n$) or Chezy number (C). These are set constant in space in the simulations presented in this paper. It is possible to enhance the effect already present in the Manning's number due to:

$$C = Mh^{1/6} \quad (8)$$

By using a more generalized form:

$$C = ah^b \quad (9)$$

This is referred to as "alluvial resistance" in MIKE 21C. The exponent b can alter the flow distribution between channels and bars.

The Saint-Venant equations are solved using a fully parallelized Alternating Direction Implicit scheme. The advection-dispersion equations are solved by using a line-implicit iteration scheme and domain decomposition. All morphological computations are fully parallelized, including trivial parallelization of calculations done in each computational cell without spatial dependencies. The hydrodynamic and morphological model components have different time-scales and have different time-step limitations. It is not feasible to apply the lowest time-step that gives stable solutions in all equations, as morphological updating can easily be 10-20 times more time-consuming than updating

the hydrodynamics. Therefore the time-scales are split by only updating the morphology at a specified frequency in order to increase the computation speed; e.g. every 10th time-step has morphological updating, which means the morphological time-step is 10 times higher than the hydrodynamic time-step. In comparison with other models such as Delft3D (Roelvink and Reniers, 2011), MIKE 21C does not apply any methodology such as a morphological factor for upscaling the morphological development.

The model is conveniently run on standard high performance servers, e.g. 16-cores XEON E5-2687W.

III SIMULATION OF BRAIDING RIVERS

III – 1 Simulation of Jamuna River

The braiding river morphology of the Jamuna River in Bangladesh is being modelled using MIKE 21C. Simulations of Jamuna River braiding river morphology were previously conducted by Enggrob & Tjerry (1998). Since then the simulations have been improved by applying increased resolution, longer model domain, and a better description of the important lateral channel migration.

The geometry inputs for the braiding simulation were a 100 km or 200 km long and 10 km wide river with initial depth of 5 m everywhere, sloping 7 cm/km (i.e. 7 m level difference over 100 km). 10 km floodplain can be added on each side with elevation 5 m above the initial river level. This floodplain merely needs to be wide enough for the river to not reach the outer edge, as this would result in very deep channels resting up against the boundary. The grid spacing is 100 m in each direction, which for 100 km length and 30 km total width amounts to 1000 by 300 grid cells.

The flow resistance can be set to different levels, which will be assimilated into the braiding pattern. For instance setting a high flow resistance causes the simulated system to become more channelized.

The hydrodynamic boundary conditions are upstream discharge set to either 45,000 m³/s (dominant discharge) or a duration curve hydrograph repeating annually. At the downstream boundary we either apply a constant water level for 45,000 m³/s or a rating curve for the duration hydrograph.

The sediment parameters are 0.16 mm uniform sand with a density of 2,650 kg/m³ and a porosity of 0.35. Sediment transport is proportional to the Engelund-Hansen formula, which has been scaled up to yield a load of 600 mill ton/year, which is the observed annual load for Jamuna River. The sediment transport is assumed to be 80% suspended load, 20% bed-load. The morphological boundary conditions are zero bed level change at the upstream end and no boundary condition at the downstream end due to the hyperbolic nature of the Exner equation.

There were no perturbations added to the initial bathymetry, but round-off errors in the computations and bank erosion will generate perturbations.

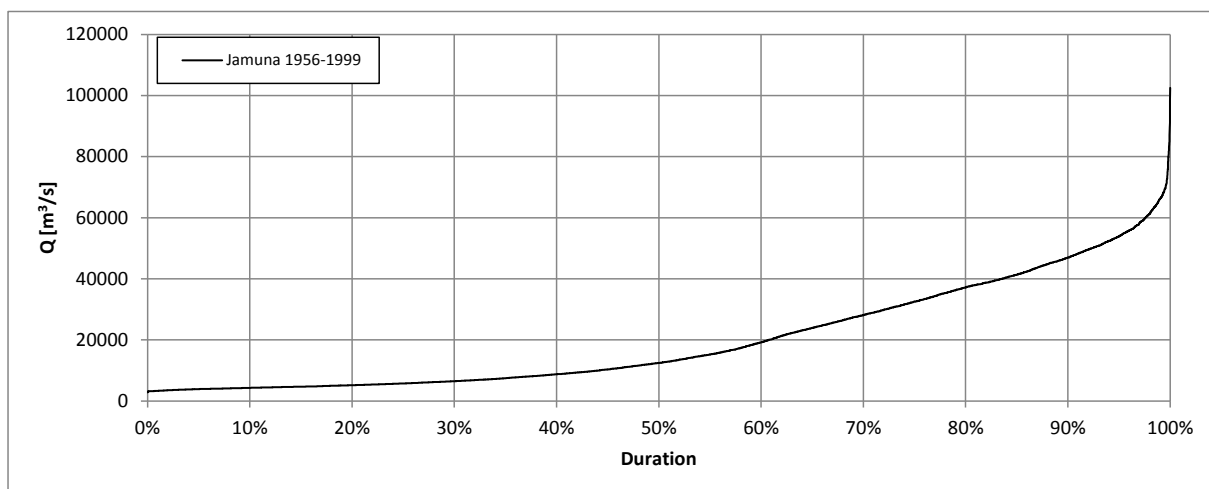


Figure 1 : Duration curve for Jamuna River based on observations 1956-1999.

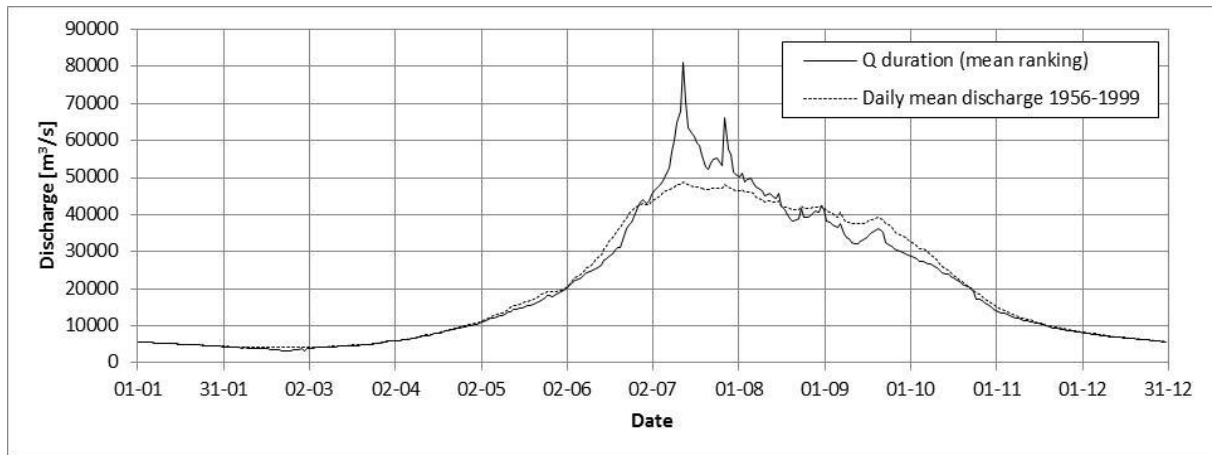


Figure 2 : Duration hydrograph for Jamuna River based on observations 1956-1999.

For simulations using a hydrograph the Jamuna River discharge time-series covering 1956-1999 was adopted with the following approach. A duration curve was developed from the data, showing the typical monsoon characteristics in Figure 1. The daily mean discharge was calculated from the data. The daily mean discharge was then combined with the duration curve to develop a duration curve hydrograph by using the ranked mean discharge as location in time for the ranked duration discharge, which gives the hydrograph shown in Figure 2. The duration curve hydrograph is repeated annually in the simulation.

First consider the situation without floodplain, as shown in Figure 3, i.e. a situation without bank erosion. The purpose of considering this case is that it shows the basic instability in the bed, while situations with bank erosion bring additional perturbations. Bank erosion is here defined by the capability of the model to erode by lateral sediment transport the banks of the river and the river is not constrained morphologically by the initial river plane. The failure of a slope via the mechanism of water flow eroding at the toe of a cut bank on a meander bend is not included in these simulations.

So the case shown in Figure 3 represents the development of the morphological instability due to the intrinsic instabilities in the numerical solution. To further simplify the situation we considered only bed-load in this case.

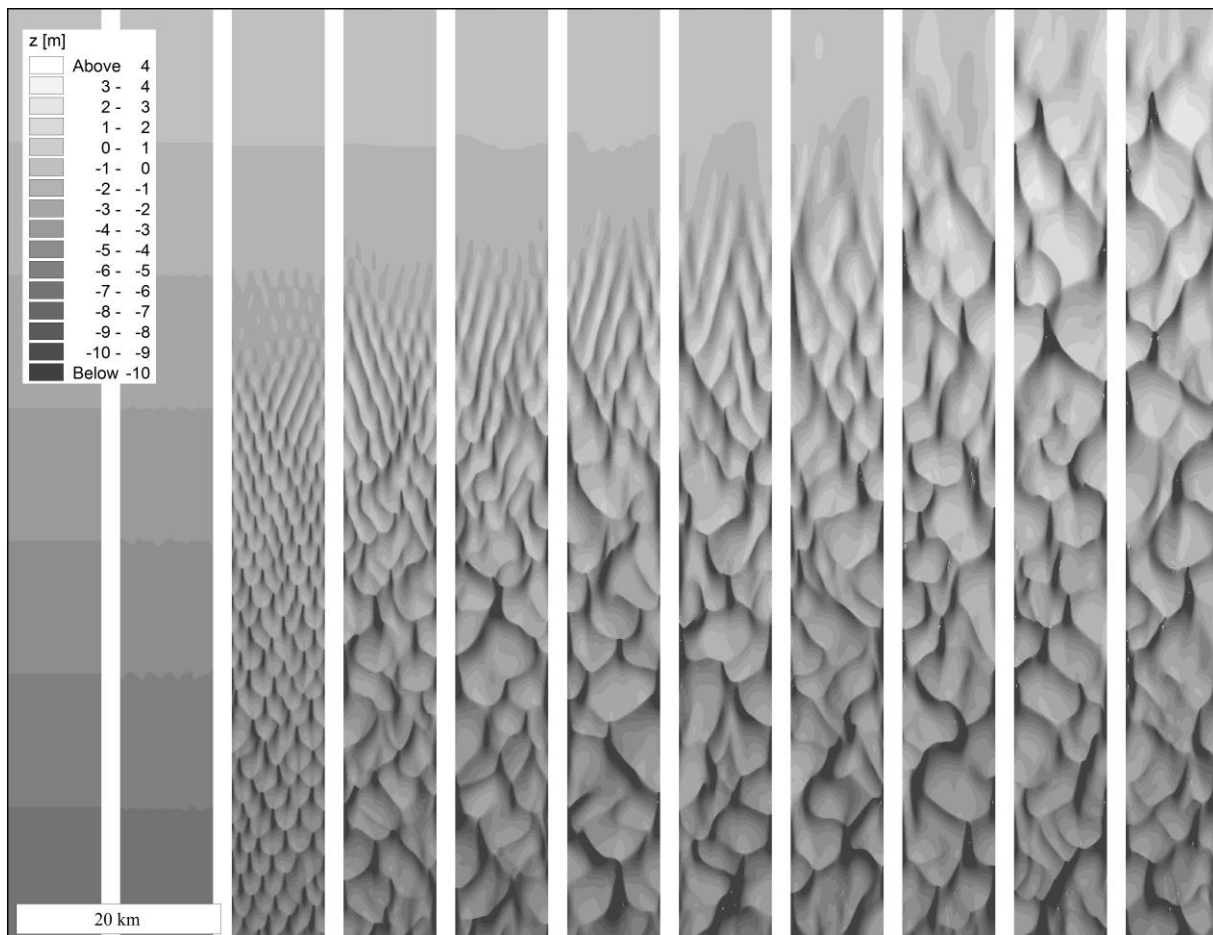


Figure 3 : Simulated development from plane bed to perturbed bed over 10 years, shown every year in the simulation period (0-10 years). Inputs: 45,000 m³/s discharge, no floodplain, bed-load only (600 mill ton/year).

The fundamental mechanism responsible for the development of braiding appears to be relatively simple: if scouring the bed locally the flow lines will contract, which will increase the sediment transport and therefore enhance scour (confluence). This cannot be sustained, and the downstream result is deposition of sediment that will lead to flow deflection (bifurcation). The braiding simulation initially develops according to this principle, but non-linear effects and interactions between confluences and bifurcations influence the matured solution.

The picture in Figure 3 is ideal for illustrating the fundamental instability, but if continuing the simulation the braiding pattern tends to freeze as very deep channels develop along the banks. For such a situation the water and sediment essentially conveys directly through these deep channels without interaction with the bed or banks, which in reality would cause significant bank erosion. It is also worthwhile noting that the initial (before it becomes strongly non-linear) development of the instability is quite different from the fully developed non-linear solution. This implies that the wave lengths for a linear stability analysis will be shorter than the mature wave lengths. It is also worth noting that the instability development initially starts a distance downstream from the inflow boundary, which is due to the fixed bed level at the boundary, but as time goes by the instability also migrates upstream.

Second consider the case where bank erosion is introduced by having a floodplain on each side of the river as well as 200 km length or a time-varying discharge, see Figure 4 (200 km length) and Figure 5 (time-varying discharge). Figure 4 shows the simulated development with a constant discharge over 20 years. After two years a braiding morphology emerges with a rather stable configuration appearing after 14-16 years.

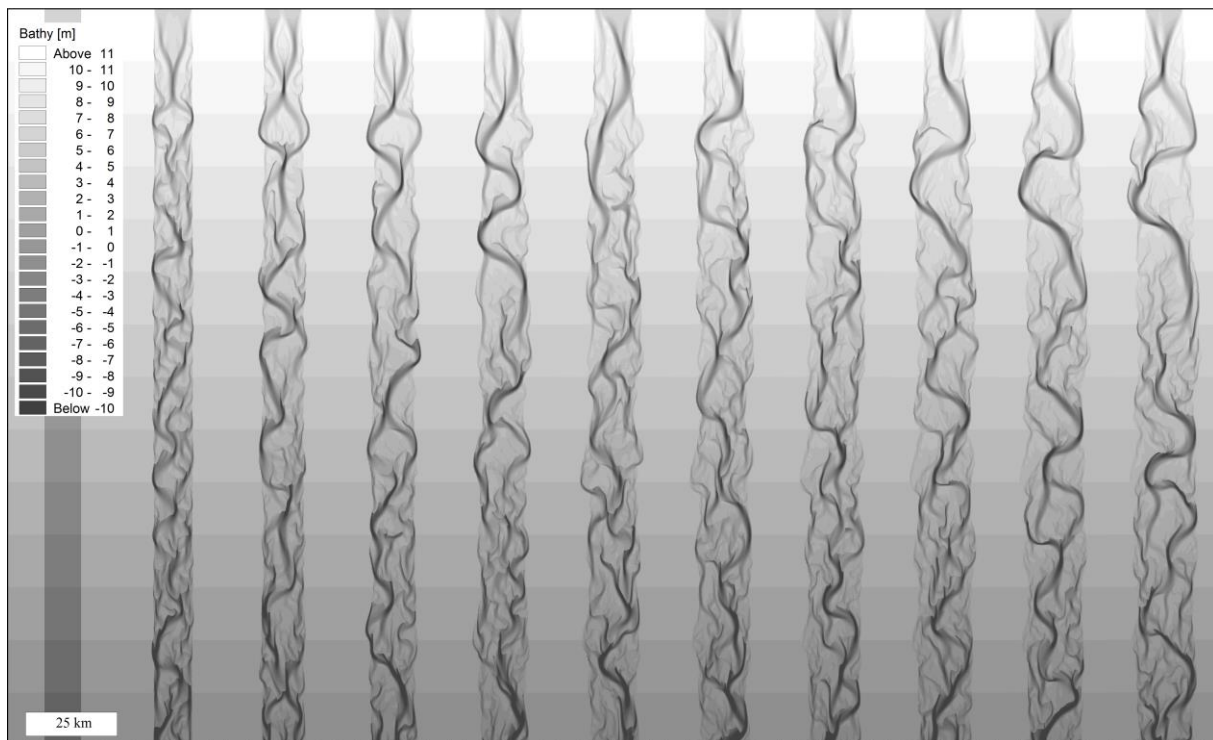


Figure 4 : Simulation of Jamuna River over 20 years shown every two years, starting from plane sloping bed, constant discharge, 200 km long model.

Figure 5 shows the solution with a time-varying hydrograph based on the duration curve. For this case only 100 km of the Jamuna River are considered as the hydrograph is computationally more demanding to simulate. The figure shows that braiding looks similar to the constant discharge simulation though the system looks stable slightly earlier around 12 years.

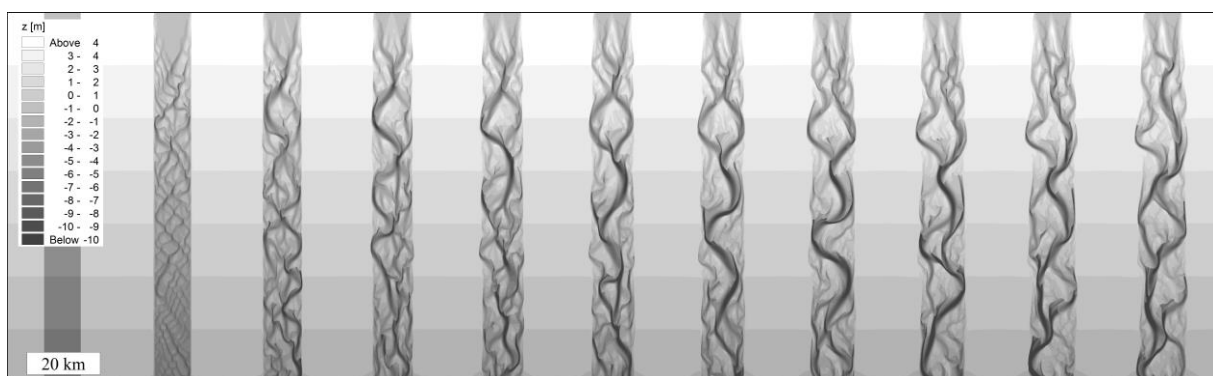


Figure 5 : Simulation of Jamuna River over 20 years with a time-varying discharge.

With respect to the critically important lateral channel migration leading to short cuts through bars, a varying discharge would seem to make the river more suited for developing a braiding morphology. It is simply easier to sustain braiding because a varying discharge will cause more flow over bars for flood conditions and adjust channels to lower sediment transport during the dry season.

Figure 6 shows comparison between simulated (left) Jamuna River plan form and the observed plan form from a satellite image. Similarities in the morphological features can be seen despite the simulation has been run under simplified conditions with respect to the time varying discharge. The longitudinal length scale of the meanders is of the same order of magnitude, while the lateral scale seems somewhat too wide. However, it should be mentioned that the lateral erosion in reality is limited by vegetation and cohesion in the banks.

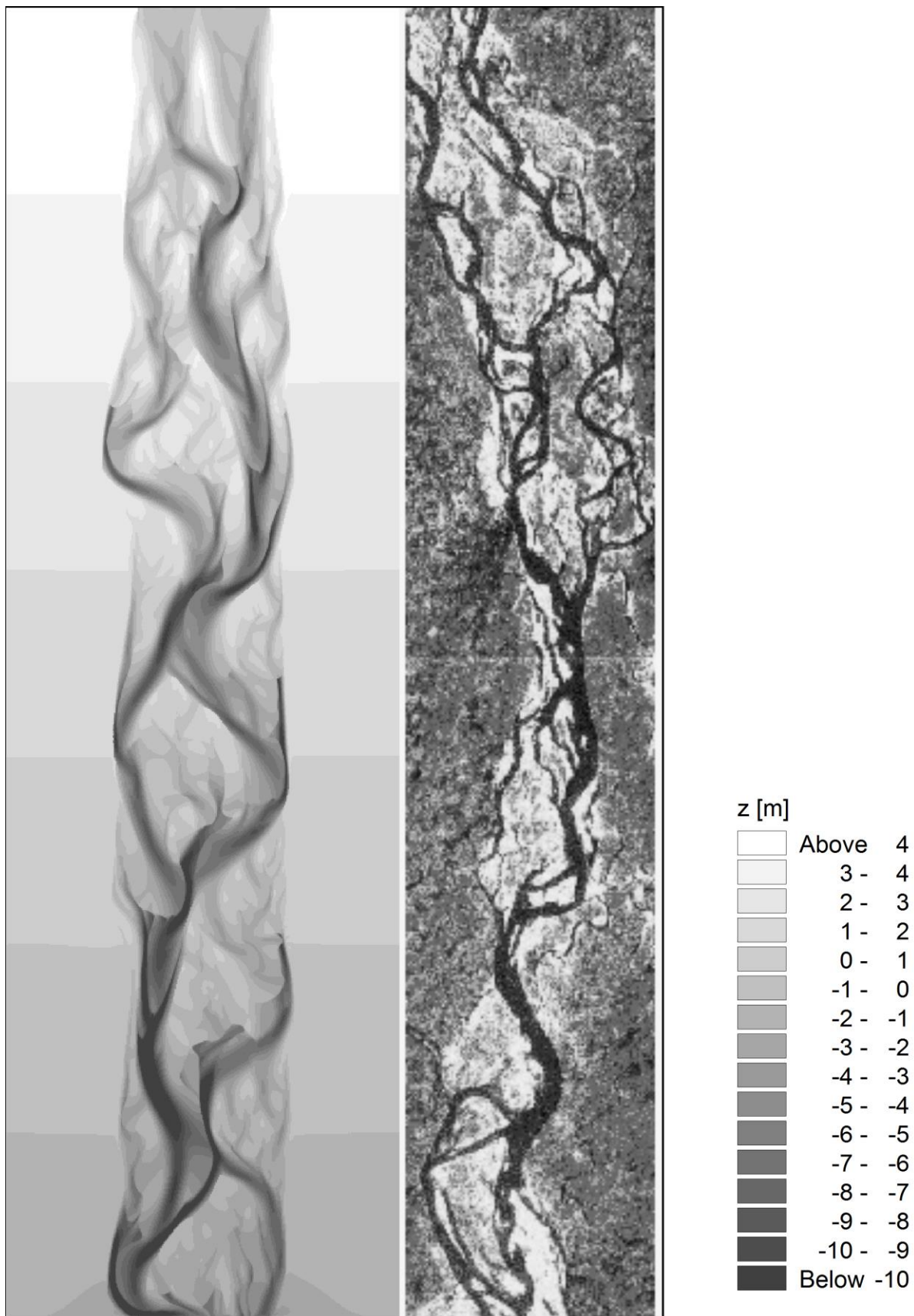


Figure 6 : Comparison between simulated (left) Jamuna River plan form and the observed plan form from a satellite image. Notice the similarities in the spatial scales.

III – 2 Sensitivity of the formation of braiding

Sensitivity tests of formation of braiding were conducted with a 100 km long Jamuna River model running over 10 years. The results are shown in Figure 7 **Error! Reference source not found.**:

1. The baseline setup with 45,000 m³/s discharge, similar to what is shown in Figure 4, except that only 100 km length is considered here.
2. Helical flow is clearly not needed for braiding to develop, but it does somewhat deprive the river of what appears to be a critical ability: lateral channel migration.
3. Reduced transverse slope effect reduces transverse channel migration, which appears to reduce braiding and can lead to a frozen channel pattern where the water and sediment is easily conveyed through the system with very low morphological activity.
4. High flow resistance makes the river attract more flow to channels and deflect from bars, which clearly leads to higher braiding intensity with smaller channels active.
5. Doubled helical flow leads to channels migrating more laterally.
6. The alluvial resistance model makes deep channels even more attractive and bars less attractive to the flow that clearly results in deeper and longer channels.
7. All sediment transport taking place as bed-load means more gravity effect on the sediment transport. This leads to a smoother solution that also appears to channelize less.

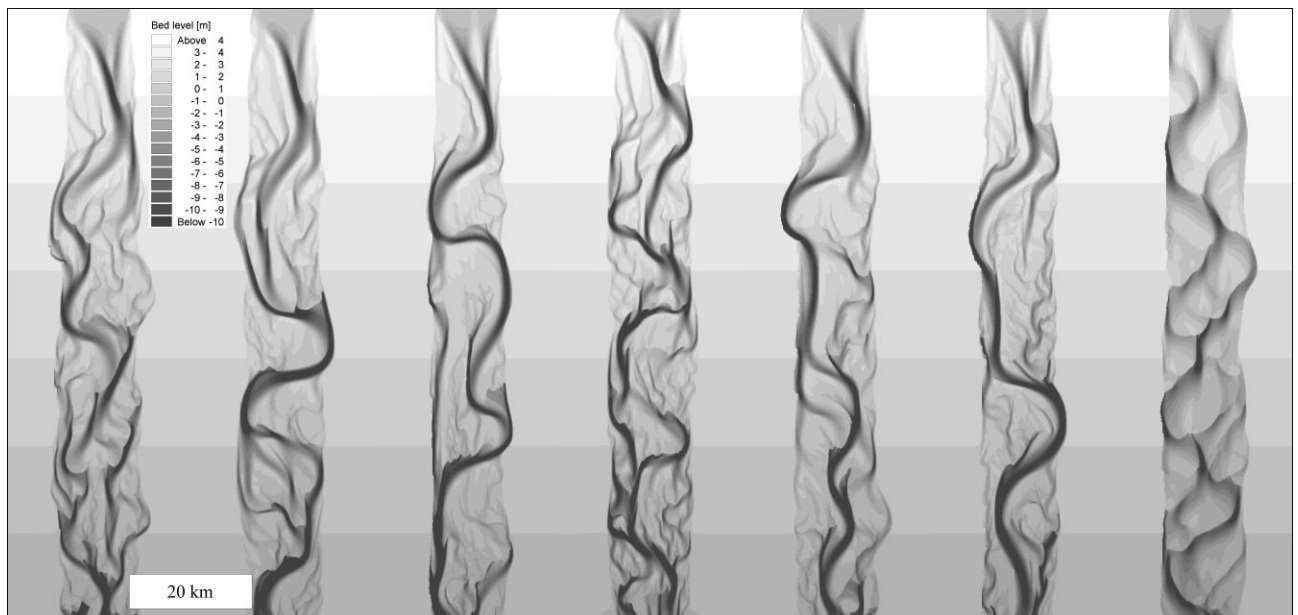


Figure 7 : Braiding sensitivity testing, from left: 1) default parameters, 2) no helical flow, 3) reduced transverse slope effect, 4) higher flow resistance, 5) doubled helical flow intensity, 6) alluvial resistance model, 7) bed-load only.

IV SIMULATION OF ESTUARINE MORPHOLOGY FORMS

IV – 1 Simulation of ebb and flood channels

Hibma (2004) successfully prepared long term morphological simulations of the formation of ebb and flood channels at time scales from decades to centuries in a theoretical tidal estuary simplified to a rectangular channel of 80 km of length and 2.5 km of width. This well-defined test case is ideal for testing the capability of MIKE 21C to simulate estuarine morphology forms.

The theoretical estuary is defined by a water depth of 15 m at the mouth and the depth decreases linearly towards the closed inland boundary. The estuary is subject to tidal movements only from a M2 tidal component with amplitude of 1.75 m. For the bottom roughness, a constant

Manning's coefficient of $0.026 \text{ s/m}^{1/3}$ is used. The bed material consists of uniform sand with $d_{50} = 240 \mu\text{m}$ and the Engelund-Hansen sediment transport formula is applied.

Similar to Hibma (2004) the estuary is schematised by a grid of 250 m by 125 m in longitudinal and transverse direction, respectively. The time step in the HD calculations is 10 seconds and the morphology is updated every 600 seconds, i.e. the bed level update is not integrated over a tidal cycle as applied in Delft3D by Hibma (2004). The initial bed-level is given small-amplitude perturbations by adding a random value to the depth value of each grid cell. These initial disturbances maximally amount to plus or minus 5% of the water depth.

The bed level development after 10, 20, 50, and 120 years of simulation is shown in Figure 8 for the middle part of the estuary. The simulation result from Hibma (2004) is also shown for comparison. It is seen that the bed level development through time is similar to Hibma (2004). After 20 years the first easily distinct morphological forms are observed. After 50 years a clear pattern of shoals with ebb and flood channels is observed. This pattern remains stable for the rest of the simulation. Deeper channels are formed along the estuary boundary, which are connected by shallower channels across the estuary. There are also distinct flood channels. The channels system repeats itself with a wavelength of about 12 km. It is emphasised that one cannot expect a one to one comparison between the two sets of results. Hibma (2004) seems to get somewhat higher deposition as compared to the present simulations. This could be explained by the difference in the updating where Hibma (2004) mentions that the higher bed levels were influenced by the application of the longer morphological time step for bed level update, whereas MIKE21 C updates the morphology throughout the tidal cycle.

The definition of the initial bed levels plays a role with respect to the time scale for development of bed forms. Simulations with MIKE 21C from a uniform sea bed resulted in a delay in the timely development where the bed forms after 50 years are comparable to the bed forms after say 30 years with a perturbed initial sea bed, i.e. delay by a factor of 2. This is not surprising considering the non-linearity in the morphological simulation.

Overall, it is reassuring that the timely development and the wave length of the channel systems are very similar in the two sets of simulation. This shows that the sediment transport in the two models must be very close despite different numerical implementations and morphological update approaches.

IV – 2 Simulation of Narmada Estuary, India

In order to further illustrate numerical modelling of estuarine morphology, the Narmada Estuary located in the Gulf of Khambhat, Gujarat, India has been simulated. The objective is to investigate if it is possible to reproduce morphological features observed in a real estuary. The estuary is not subject to substantial dredging except near the mouth, while the construction of upstream dams has changed the freshwater flow and sediment load. Thus the estuary is today subject to erosion and morphological changes. Simulating the historical build-up/erosion of the estuary requires information of previous estuary and river bed, river run-off and sediment load, and how this has changed due to construction of water reservoirs. As the objective is to investigate if the model can simulate observed main morphological features, the focus is on the redistribution of sediments within the estuary on the time scale of years.

Narmada Estuary is macro-tidal with a mean tidal range of 8.6 m at the mouth. The tide propagates about 90 km up the river. The freshwater run-off is predominantly during the monsoon from June-September. With the construction of various dams the reservoir storages have reduced the peak flows considerably. In the pre-dam scenario, the annual peak flow was about $80,000 \text{ m}^3/\text{s}$. This has today decreased considerably. In the presented simulation a peak flow of about $13,000 \text{ m}^3/\text{s}$ is assumed, which occurs during the month of September. The estuary is characterised by clay/silt/fine sand sediments so in the simulations a grain size of 0.18 mm with $2,650 \text{ kg/m}^3$ density and porosity of 0.35 is applied with the Engelund-Hansen sediment transport formula.

The model is forced by the astronomical tide at the mouth and the yearly river discharge at the upstream boundary with a low flow of about $300 \text{ m}^3/\text{s}$ and a peak flow of $13,000 \text{ m}^3/\text{s}$. The computational grid is shown in Figure 9 with zooms of the curvilinear grid. The model covers an area of approximately 90 km along the estuary. The width of the mouth is about 10 km. The straight upper

part is an artificial extension to include the propagation of the tide within the model domain. The model domain is defined by 68 cells across the mouth, 25 cells across the river at the upstream end, and 604 cells along the estuary. The hydrodynamic time step is 5 seconds. The sediment transport and update of morphology is done for each 5 minutes (60 times the hydrodynamic time step). The initial bed level is set to the average depth of the estuary (1.16 m relative to chart datum), except for a narrow stretch across the mouth where the depths are set equal to 2 m. The model has been run for a period of 30 years. A close-up view of the simulated lower estuary bed levels are shown in Figure 10 after 5, 10 and 30 years together with the actual bed levels observed in 2008. The simulations show that already after 5 years the main morphological features emerge. Tidal channels and shoals/islands develop in a pattern that resembles the observed bathymetry. However, the model exaggerates the flow south of the main island in the middle of the figure, which today is a dead branch. Similarly the model underestimates the flow in the upper bend where a deep channel exists. Further in the simulation tidal channels develop in the narrower part of the estuary, which shift from bank to bank in a manner as observed in the schematic estuary. Relics of such a pattern can be seen in the observed bathymetry although the north bank is the main channel today. Towards the mouth tidal channels and shoals appear but as time progresses the simulation show signs of sediment starvation. This shows that the marine sediment inflow is underestimated in the model. Overall it is emphasised that a direct comparison with the existing bathymetry is not possible. The simulation is made with a yearly run-off that is repeated for each year and the impact of sediment transport further into the Gulf of Khambat is not included. Nevertheless the simulation reproduced morphological features that also can be observed in nature.

The 30 years simulation was prepared with a river run-off with a peak flow once per year. In order to investigate the importance of the river flow relative to the tidal forcing a simulation has been made with a peak flow of $13,000 \text{ m}^3/\text{s}$ every month. With a monthly peak flow the estuary will experience 30 peak flows in 2.5 years.

In Figure 11 the simulated results with a monthly peak discharge after 2.5 years are compared with the simulated results after 30 years but with a yearly peak discharge. For reference also shown is the observed bathymetry in 2008. The 30 years simulation shows sign of too low sediment input and indicates that the tide gradually becomes stronger and builds deeper channels. For the 2.5 years results the formation of shoals seem more pronounced as the erosive force from the tide is less.

The 2.5 years bed levels also show morphological features that can be recognised in the observed 2008 bathymetry. For example there is a tendency to create a flood channel in the upper bend in the middle of the estuary.

It should be mentioned that the results of the simulations of Narmada depend on the definition of the initial bed levels, the hydrodynamic forcing and the sediment load. However, with a realistic forcing the longer the simulation the less important the initial conditions are, see Vested et al. 2013.

The actual bed levels depends on the timing and history of forcing events, which in practice is major challenge in morphological predictions as it requires extensive simulations with many combinations of forcing.

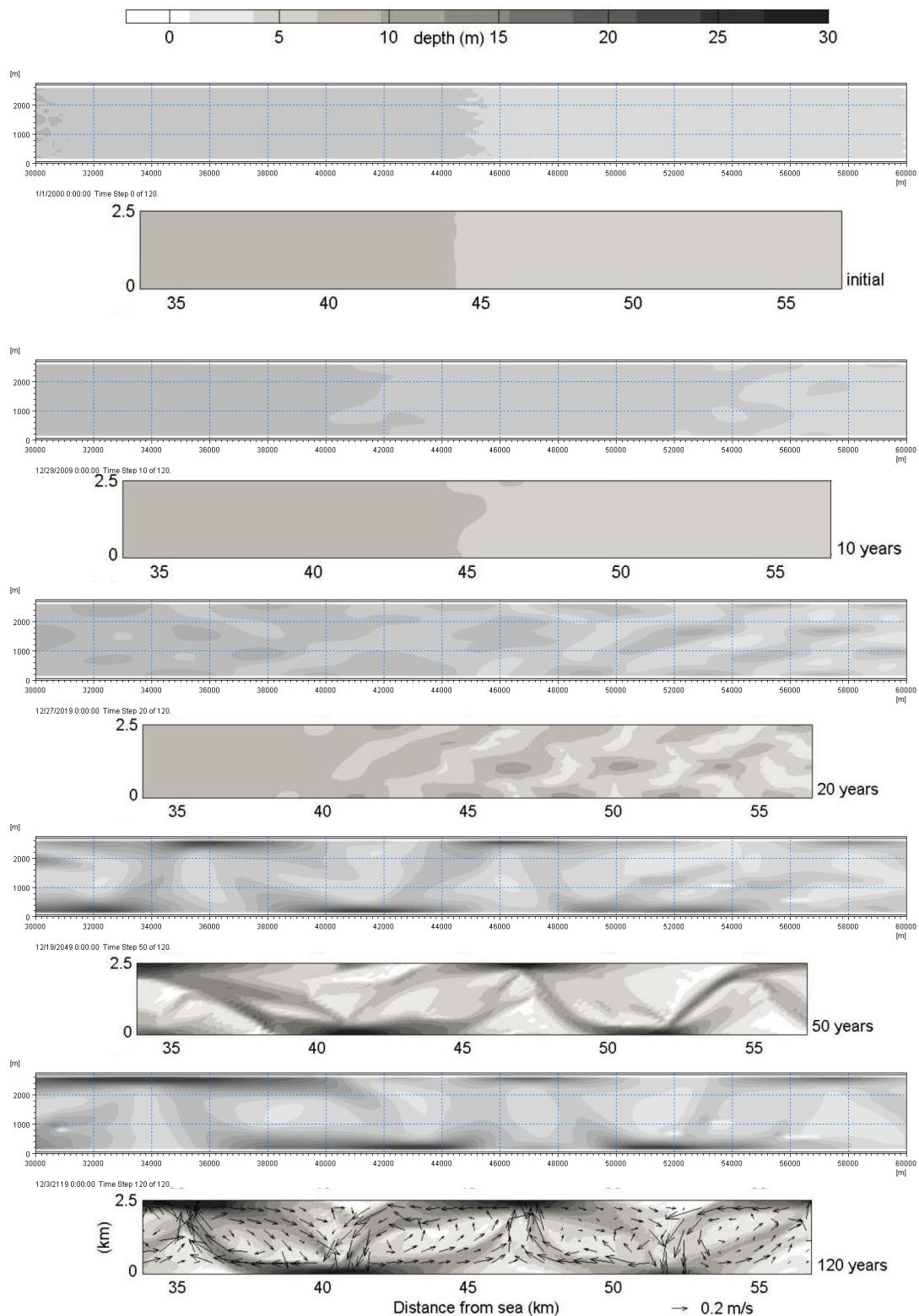


Figure 8: Comparison between MIKE 21C and Hibma ((2004), reproduced from figure 5.3 of thesis)) simulated bed levels. The panels show the middle section of the estuary. Upper panel and lower panels show MIKE 21C and Hibma (2004) results, respectively. The first panel indicate the depth contour legend.

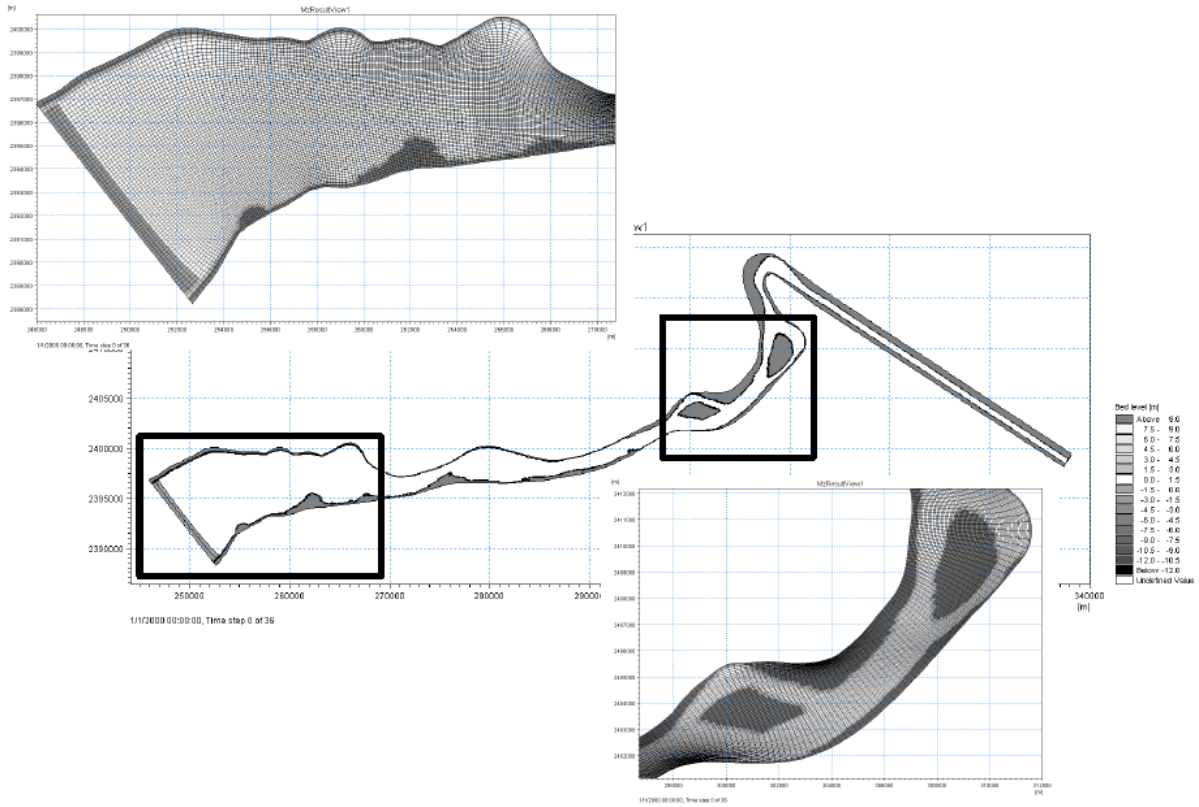


Figure 9: Model domain and computational grid for Narmada Estuary with zooms examples of the curvilinear grid. Initial bed level is 1.16m.

The differences between the present two sets of results also suggest that the actual existing bathymetry is the result of historically varying river discharges and sediment loads in combination with the tidal flow and sediment input from off-shore.

From a modelling point of view the results also demonstrate that one should be extremely careful in attempts to upscale the river discharge and sediment input in order to speed up the long term simulations.

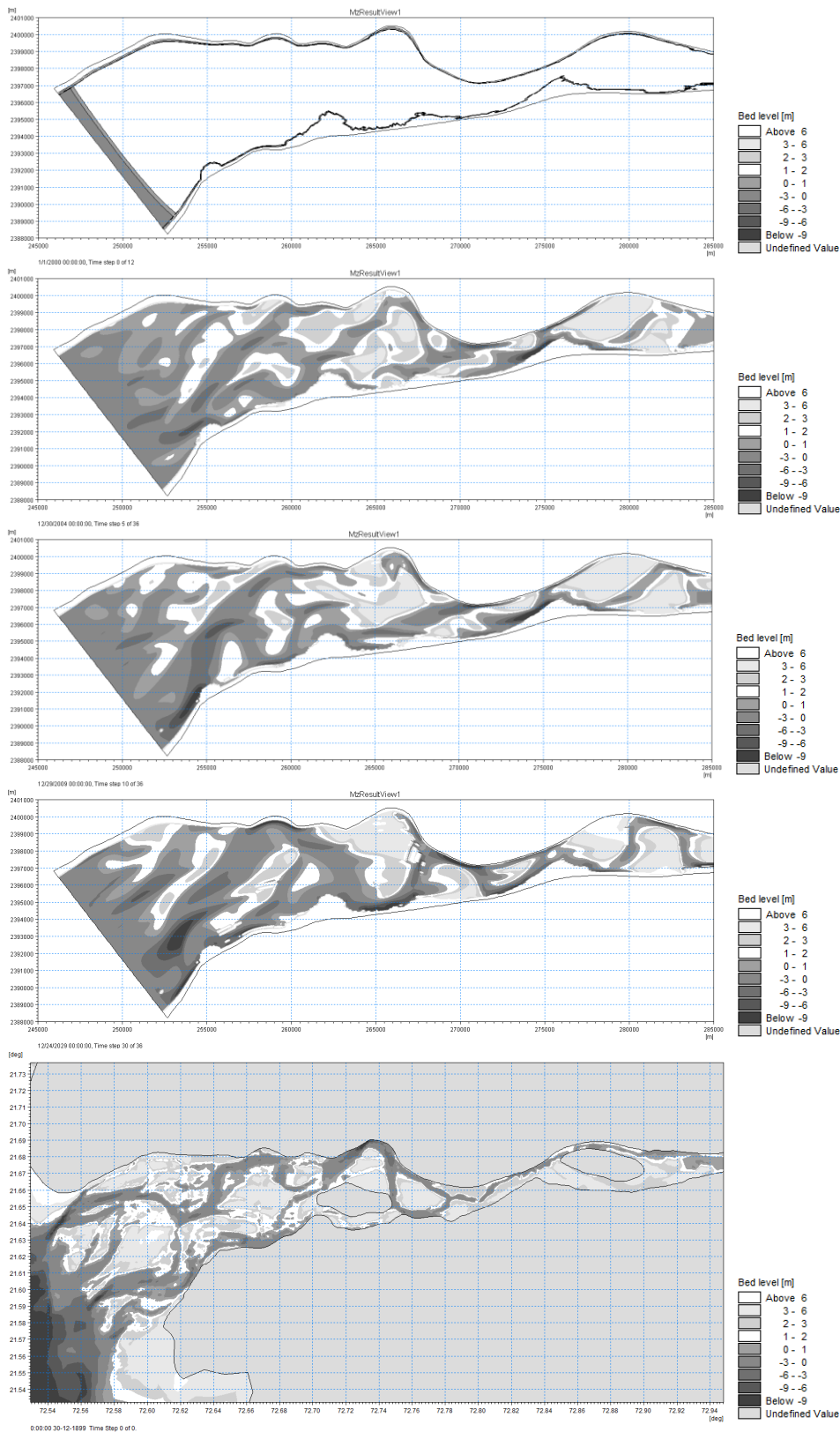


Figure 10: Lower Narmada estuary. From top to bottom, initial bed level, 5, 10 and 30 years of simulated bed level with a low flow of $300 \text{ m}^3/\text{s}$ and peak river flow of $13,000 \text{ m}^3/\text{s}$ repeated each year. The lowest panel shows the bed level surveyed in 2008.

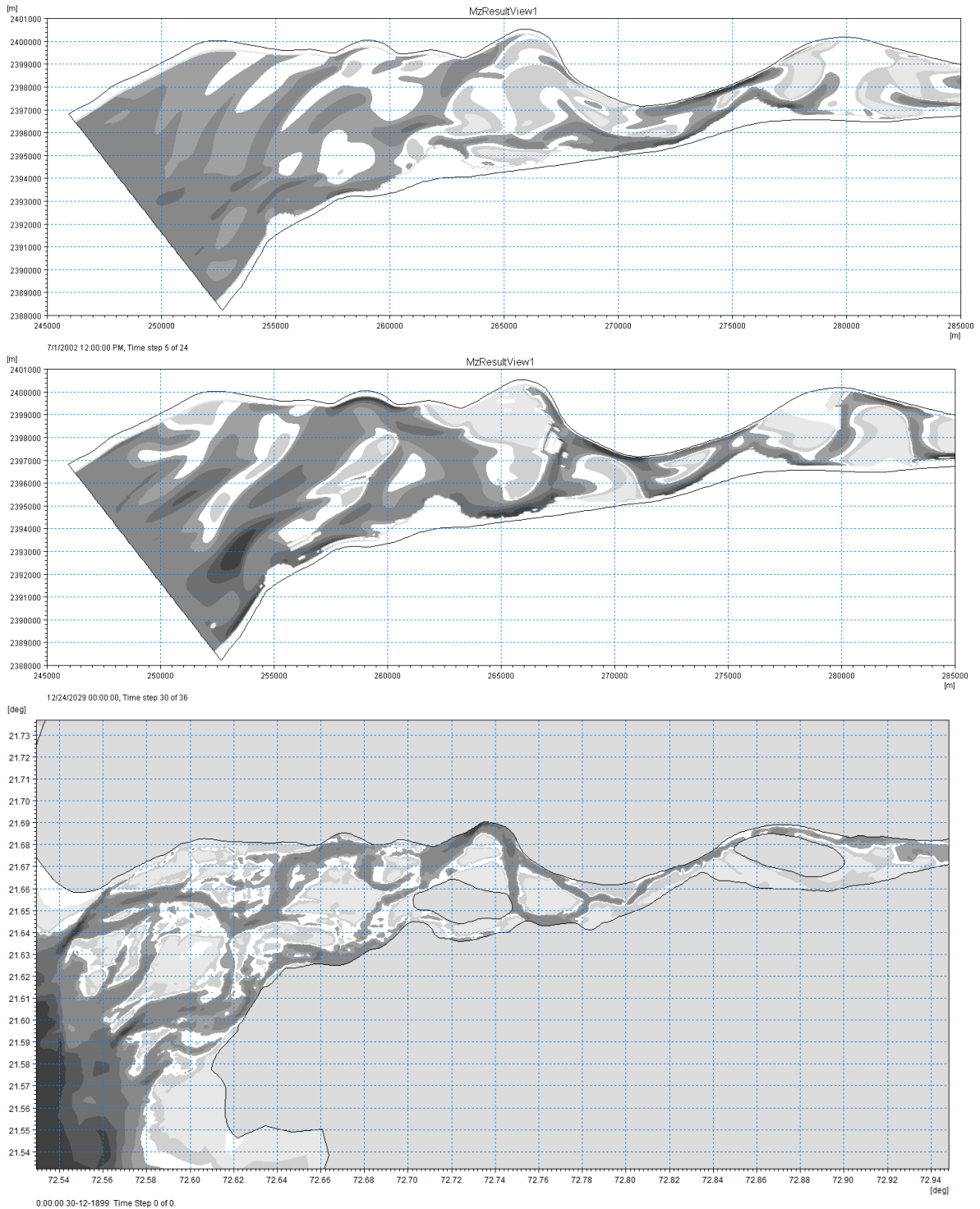


Figure 11 : Lower Narmada estuary. Importance of river flow relative to tidal forcing. Upper panel shows simulated bed level after 2.5 years with monthly peak river flow and middle panel is for 30 years of simulation but with a yearly peak flow. The lowest panel is the bed level surveyed in 2008.

V CONCLUSIONS

The various simulations of braiding river morphology point towards the following conclusions: Braiding seems to develop from flow attraction to channels (confluences) and deflection from bars (bifurcations). Furthermore the onset of braiding from a plane bed appears to be very robust and will trigger in all considered scenarios, although with varying scales. In rivers a time-varying

discharge is not required for braiding to develop but it appears as if a varying discharge makes it easier to sustain braiding. This is probably due to more varied flows over the bars. The flow resistance model influences braiding by changing the flow distribution between channels and bars, i.e. the more attractive channels are to the flow compared to bars the easier it is to develop braiding. Braiding needs lateral channel migration to be sustained; if channels do not migrate laterally the braiding pattern tends to freeze in space and time.

A sufficiently wide river is critical for simulated braiding to be sustained. One reason for this is that a wide river makes it easier for short cuts to develop over bars when channels migrate laterally. Without these short cuts the simulated braiding pattern will freeze. This behaviour was also reported by Hibma (2004), although for a simulated estuarine system.

In tidal flow systems, the development of instabilities triggering formation of braiding seems weaker. This may be because the net sediment transport is smaller compared to rivers. Introduction of random noise in the bed level can speed up the formation of channels and shoals with time scales similar to those found by Hibma (2004). Attempts to upscale the morphological development by enhancing the river flow in combined tidal and river flow is not recommendable.

Overall realistic natural morphological features can be reproduced with the MIKE 21C model, thus can be applied to assess long term impact and predict future bed levels. However, the basic chaotic behaviour of braiding means no single simulation represents the truth but rather one of many. This calls for an ensemble approach similar to what is applied in complex chaotic systems such as in weather forecasting. Such multi-simulation forecasting approaches are still limited in practical application by the computational resources available.

VI ACKNOWLEDGMENTS AND THANKS

The authors would like to thank Dr. Mark Schmelter , Chief Engineer Water Resources, Freeport-McMoRan for many discussions on river and estuary morphology.

Discharge time-series and sediment transport data for the Jamuna River were provided courtesy of Dr. Kazi Iqbal Hassan. Dr. Kim Wium Olesen and Mr. Hans Enggrob are acknowledged for always being willing to take on technical discussions.

VII REFERENCES AND CITATIONS

- Engelund, F. and Hansen, E. (1967) *A monograph on sediment transport in alluvial streams*, Teknisk Forlag, Copenhagen, Denmark: Danish Technical University
- Olesen, K.W. (1987) *Bed topography in shallow river bends*, Faculty of Civil Eng., Delft Univ. of Tech., Report 87-1, 1987
- Ahmadi, M.M., Ayyoubzadeh, S. A., Montazeri Namin, M., and Samani, J. M. V. (2009) *A 2D Numerical Depth-averaged Model for Unsteady Flow in Open Channel Bends*, J. Agr. Sci. Tech. (2009) Vol. 11: 457-468
- H. J. de Vriend, J. Dronkers, M. J. F. Stive, A. V. Dongeren, and Z. B. Wang. (January 2002) *Coastal inlets and tidal basins (partly in Dutch)*. TU Delft Repository
- Enggrob H.G. and Tjerry S. (1998) *Simulation of Morphological Characteristics of a Braided River*. River, Coastal and Estuarine Morphodynamics(RCEM) Proceedings 1998
- Hibma A. (2004) *Morphodynamic modelling of Estuarine channel-shoal systems*. Phd Thesis Technical University Delft 2004.
- Galappatti, R. (1983) *A depth integrated model for suspended transport*, Communications on Hydraulics, Vol. 83-7, Delft University of Technology, Delft, 114p.
- Roelvink, D. and Reniers, A. (2011) *A Guide To Modeling Coastal Morphology* (Advances in Coastal and Ocean Engineering). World Scientific
- Rijn, L.C. van (1984) *Part I Bedload transport*, J.Hyd.Eng,110, Oct. 1984
- Rijn, L.C. van (1984) *Part II Suspended load transport*, J.Hyd.Eng,110, Oct. 1984
- Vested, H.J., Tessier, C., Christensen, B.B., and Goubert, E. (2013): *Numerical modelling of morphodynamics – Vilaine Estuary*, Ocean Dynamics (2013) 63: pp 423-446